Journal of Fluorescence, Vol. 4, No. 4, 1994

Fluorescence Intensity and Anisotropy Decays of the DNA Stain Hoechst 33342 Resulting from One-Photon and Two-Photon Excitation

Ignacy Gryczynski[1] and Joseph R. Lakowicz[1]

Received October 18, 1993

We examined the steady-state and time-resolved fluorescence spectral properties of the DNA stain Hoechst 33342 for one-photon (OPE) and two-photon (TPE) excitation. Hoechst 33342 was found to display a large cross section for two-photon excitation within the fundamental wavelength range of pyridine 2 and rhodamine 6G dye lasers, 690 to 770 and 560 to 630 nm, respectively. The time-resolved measurements show that intensity decays are similar for OPE- and TPE. The anisotropy decay measurements of Hoechst 33342 in ethanol revealed the same correlation times for TPE as observed for OPE. However, the zero-time anisotropies recovered from anisotropy decay measurements are 1.4-fold higher for TPE than for OPE. The anisotropy spectra of Hoechst 33342 were examined in glycerol at −20°C, revealing limiting values close to the theoretical limits for OPE (0.4) and TPE (0.57). The steady-state anisotropy for OPE decreases in the shorter-wavelength region (R6G dye laser, 280–315 nm), but the two-photon anisotropy for 560 to 630-nm excitation remains as high as in the long-wavelength region (690–770 nm). This result suggests that one-photon absorption is due to two electronic transitions, but only one transition contributes to the two-photon absorption over the wavelength range from 580 to 770 nm. Our demonstration of these favorable two-photon properties for Hoechst 33342, and the high photostability of the dye reported by other laboratories, suggests that this dye will be valuable for time-resolved studies of DNA with TPE and for two-photon fluorescence microscopy.

KEY WORDS: Hoechst 33342; one-photon excitation; two-photon excitation; anisotropy decay; time-resolved fluorescence; frequency-domain; DNA.

INTRODUCTION

The chromatin stain Hoechst 33342[2] binds to DNA with a significant increase in fluorescence [1–3]. The ease of DNA staining by Hoechst 33342, and the bright fluorescence of the dye–DNA complex, has resulted in the widespread use of Hoechst 33342 in fluorescence microscopy [4,5], flow cytometry [6,7], and chromosome analysis [8–10]. Recent reports have provided detailed information of the interactions of Hoechst 33342 with DNA. It is now known from X-ray crystallography [11] and NMR spectroscopy [12–14] that Hoechst 33342 binds in the minor groove of DNA and specifically interacts with an AATT sequence.

In the past several years, there has been increased interest in the use of two-photon excitation (TPE) of biological molecules. By TPE we mean the simultaneous absorption of two long-wavelength photons to excite the

[1] Center for Fluorescence Spectroscopy, Department of Biological Chemistry, University of Maryland School of Medicine, 108 North Greene Street, Baltimore, Maryland 21201.

[2] Abbreviations used: bis(MSB), p-bis(*O*-methylstyryl)benzene; DAPI, 4',6-diamidino-2-phenylindole, hydrochloride; HOE, Hoechst 33342, bis-benzimide, 2,5'-bi-1H-benzimidazole, 2'-(4-ethoxyphenyl)-5-(4-methyl-1-piperazinyl); OPE, one-photon excitation; TPE, two-photon excitation.

1053-0509/94/1200-0331$07.00/0

fluorophore to the lowest excited-singlet state (S_1). TPE has been applied to tryptophan and proteins [15,16], to labeled membranes [17], and to DNA stained with DAPI [18], as well as to analytical chemistry [19,20] and to analysis of the electronic spectra of biomolecules [21–23]. An important new application of TPE is in fluorescence microscopy [24,25]. This use of TPE results in an ability to obtain confocal fluorescent images because TPE occurs mainly at the focal point of the incident light where the intensity is highest. Hence, we questioned whether Hoechst 33342 would display a good cross section for TPE and how the lifetimes, correlation times, and anisotropy spectra would depend on one-photon excitation (OPE) or TPE. Such information is needed to interpret the two-photon images and for the use of Hoechst 33342 in the emerging technology of fluorescence lifetime imaging [27,28].

MATERIALS AND METHODS

Calf thymus DNA was obtained from Sigma, and Hoechst 33342 from Molecular Probes, and used without further purification. To accelerate dissolving, the DNA was sonicated for 10 min in an ice bath, followed by centrifugation for 30 min at 10,000 rpm to remove particles. The buffer was 10 m*M* Tris, pH 8. The DNA concentration, as millimolar base pairs, was calculated using a 13,500 M^{-1} cm^{-1} at 259 nm, and the concentration of Hoechst 33342 was calculated using 42,000 M^{-1} cm^{-1} at 348 nm for the free form [29].

One- and Two-Photon Excitation

To facilitate comparison of the data, the OPE and TPE experiments were performed on the same solution, containing 1 m*M* base pairs (bp) DNA and 0.01 m*M* Hoechst 33342, for a 100/1 bp/HOE ratio. Under these conditions, all the fluorophore molecules appear to be bound and the intensity decays are independent of the bp/HOE ratio. The concentration of HOE in glycerol was 0.01 m*M*.

For both OPE and TPE, the emission was observed through a 460-nm interference filter with an approximate 12-nm bandpass. Emission spectra were measured using a monochromator with 2-mm slits, yielding a 10-nm bandpass.

For the one-photon measurements, we used 0.5 × 0.5-cm cuvettes with excitation and emission near a corner of this smaller cuvette. This cuvette was positioned off center in a 1 × 1-cm cuvette holder. For the two-photon measurements, we used 1.0 × 0.5-cm cuvettes, with the long axis aligned along the incident light path and with the focal point positioned about 0.5 cm from the surface facing the incident light. The position of the cuvette was adjusted so that the excitation laser beam crossed the solution near the observation window.

OPE from 282 to 312 nm was accomplished using the frequency-doubled output of a rhodamine 6G (R6G) dye laser and from 350 to 385 nm using the frequency-doubled output of a pyridine 2 dye laser. TPE from 564 to 630 and 700 to 770 nm was accomplished with the fundamental output of these dye lasers, respectively. The dye lasers were synchronously pumped with the 514-nm output of a mode-locked argon ion laser, and cavity-dumped at 3.795 MHz. Signals from the solvents alone were less than 0.5% for both OPE and TPE. The excitation beam was focused by using a 5-cm-focal length lens. A similar lens was used for the collection of the fluorescence. Steady-state anisotropy spectra were obtained in the usual L-format manner by measuring the intensity of the parallel and perpendicular components of the emission, with correction for the *G* factor, which was close to unity.

Time-Dependent Intensity and Anisotropy Decays

Frequency-domain intensity and anisotropy decays were obtained on the gigahertz instrument described previously [30,31]. Intensity decays [$I(t)$] were fit to the multiexponential model using

$$I(t) = \sum_i \alpha_i \exp(-t/\tau_i) \quad (1)$$

where α_1 are the amplitudes associated with the decay time τ_i. The differential phase and modulated anisotropy data were fit to the multicorrelation time nonassociated anisotropy decay [$r(t)$] model

$$r(t) = \sum_j r_{0j} \exp(-t/\theta_j) \quad (2)$$

where r_{0j} is the portion of the total anisotropy ($r_0 = \Sigma r_{0j}$) which decays with a correlation time θ_j. The intensity and anisotropy decay laws were recovered by least-squares analysis of the frequency-domain data. In the case of the anisotropy decays, the uncertainty in phase and modulation were taken as 0.2° and 0.005, respectively.

RESULTS

Emission Spectra

Emission spectra of Hoechst 33342 in ethanol are shown in Fig. 1. The same emission spectra were ob-

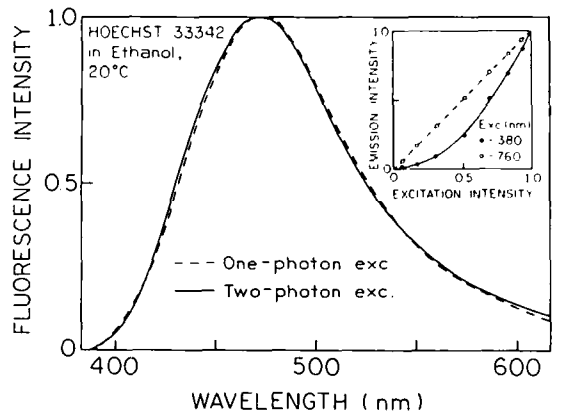

Fig. 1. Fluorescence emission spectra for one-photon (– – –; 380 nm) and two-photon (——; 760 nm) excitation of Hoechst 33342 in ethanol. The inset shows the dependence of the intensity on the incident light level, normalized to that observed for the highest incident light level.

served for OPE (– – –) and TPE (——) excitation at 380 and 760 nm, respectively. The emission was quadratically dependent on the incident intensity at 760 nm (●), but linearly dependent on intensity at 380 nm (○) (Fig. 1, insert). The emission intensities (inset) were normalized to unity for the maximum excitation intensity, so that the intensities for OPE and TPE cannot be directly compared.

This quadratic intensity dependence is strong evidence that the observed emission was in fact due to simultaneous absorption of two photons at 760 nm. The fact that the emission spectra are identical for OPE and TPE indicates that emission occurs from the same state, irrespective of the mode of excitation. Similar results were obtained for HOE bound to DNA (not shown), which also showed a quadratic dependence on intensity for TPE, and identical emission spectra for OPE and TPE.

The use of Hoechst 33342 as a two-photon probe requires a usefully high cross-section for two-photon absorption. We estimated the two-photon cross section for HOE by comparison with bis(MSB), which has a known two-photon cross section and the largest cross section known at this time [26]. Based on this comparison, using an excitation wavelength of 580 nm, we estimated the two-photon cross section of HOE to be about 2×10^{-48} cm^4 s/photon molecule, which compares very favorably with bis(MSB), with a value of 6.9×10^{-48} cm^3 s/photon molecule [26]. Hence, Hoechst 33342 can be expected to be a useful two-photon probe in both fluorescence spectroscopy and microscopy.

Fluorescence Intensity Decays

We questioned whether HOE would display the same decay time(s) for OPE and TPE. Frequency-domain intensity decay data are shown in Fig. 2 for HOE in ethanol (left) and when bound to DNA (right). In ethanol the decay of HOE is a single exponential, 3.3 ns, independent of OPE or TPE. When bound to DNA the intensity decay of HOE is weakly multiexponential. While slightly different α_i and τ_i values were found for OPE and TPE, we believe that the minor difference between the OPE and the TPE decay is due to experimental error. In total, the data in Fig. 2 suggest that the intensity decay of HOE is not dependent on the mode of excitation.

Frequency-Domain Anisotropy Decays

The frequency-domain anisotropy data are distinct for OPE and TPE of Hoechst 33342 in ethanol (Fig. 3)

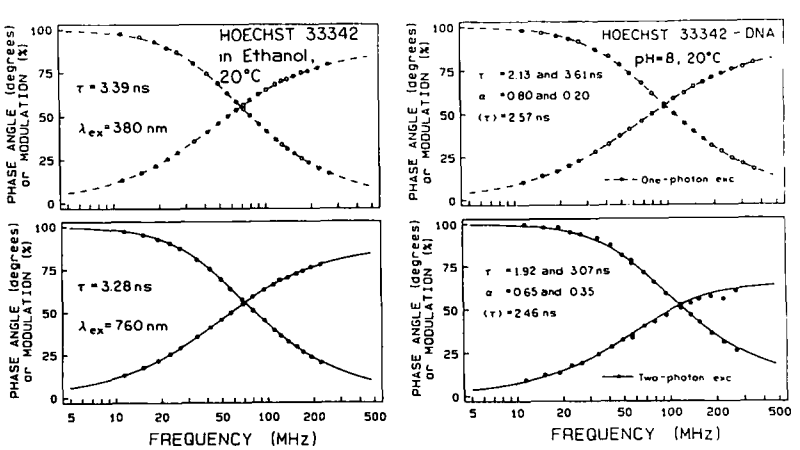

Fig. 2. Frequency-domain intensity decays for Hoechst 33342 in ethanol and when bound to DNA for OPE (○; top) and TPE (●; bottom).

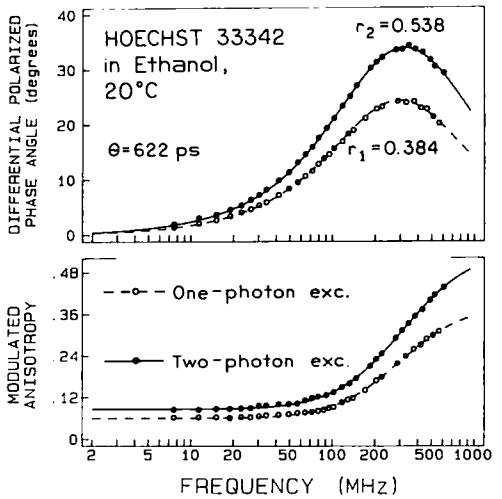

Fig. 3. Differential polarized phase angles for Hoechst 33342 in ethanol at 20°C, obtained for one-photon (○) and two-photon (●) excitation.

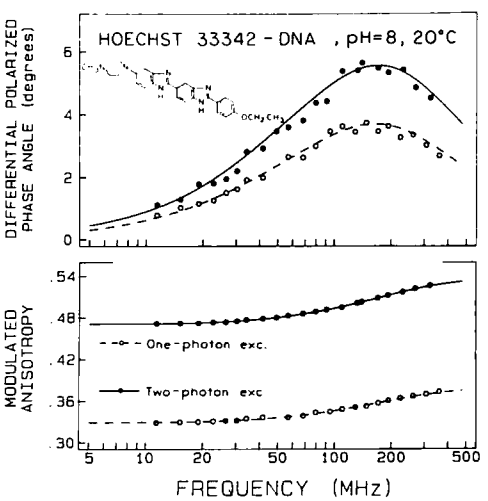

Fig. 4. Frequency-domain anisotropy data for OPE (○) and TPE (●) of Hoechst 33342-DNA.

and in Hoechst DNA complex (Fig. 4). The differential phase and modulated anisotropy values are higher for TPE (●) than for OPE (○). This effect is reminiscent of our previous results for diphenylhexatriene (DPH), 2,5-diphenyloxazole (PPO), and DAPI [17,18,32]. In the case of DPH and PPO, we found that the anisotropy values for OPE and TPE were related by a factor of 10/7, indicating that all of the off-diagonal elements in the two-photon transition matrics are zeros. The TPE anisotropy values are higher than the OPE values due to an apparent $\cos^4\theta$ photoselected for TPE. The fact that the time 0 anisotropies r_0 are linked by the factor 10/7 can

Table I. Correlation Time Analysis of the Hoechst 33342 in Ethanol at 20°C

Excitation (nm)	r_0	θ (ns)	χ^2_R
380, OPE	0.384	0.626	1.9
760, TPE	0.539	0.619	3.2
Global, OPE and TPE	0.384 and 0.538	0.621	2.6

Table II. Multicorrelation Time Analysis of the Hoechst 33342–DNA Complex

Excitation (nm)	n^a	$r_0 g_i$	θ_i (ns)	χ^2_R
380, OPE	1	0.366	18.9	32.2
	2	0.067	1.4	
		0.314	85.8	1.0
760, TPE	1	0.519	20.1	97.9
	2	0.090	1.4	
		0.450	79.6	1.2
Global, OPE and TPE	1	0.365, 0.519	19.9	64.6
	2	0.066, 0.090	1.4	
		0.315, 0.450	80.8	1.1

[a]Number of components in multiexponential fits.

be seen from the global analyses in Tables I and II. In this global program, the r_0 values are forced to be related by this factor. The fact that the χ^2_R values for the global OPE and TPE analysis remains low indicates that the data satisfy this relationship. Importantly, the correlation times are identical for OPE and TPE. This suggests that there are no adverse affects and/or local heating due to the intense illumination at 760 nm. Additionally, the simple linkage of the one- and two-photon anisotropy values allows the direct comparison of the resulting for one- and two-photon experiments.

The higher r_0 values for TPE facilitate the resolution of more complex anisotropy decays. This can be seen from the χ^2_R surfaces for r_0 and the correlation time (θ) of HOE in ethanol (Fig. 5). The χ^2_R values for TPE (——) are more strongly dependent on the parameter values than are the χ^2_R data for OPE (— — —).

Anisotropy Excitation Spectra of Hoechst 33342 in Glycerol at −20°C

In fluid solution (ethanol) and when bound to DNA, the anisotropy values of HOE are decreased by rotational diffusion. A more accurate comparison of the anisotropy values for OPE and TPE can be obtained from measurements of the anisotropy values in the absence of diffusion. This was accomplished by measurement of the excitation anisotropy spectra of HOE in glycerol at

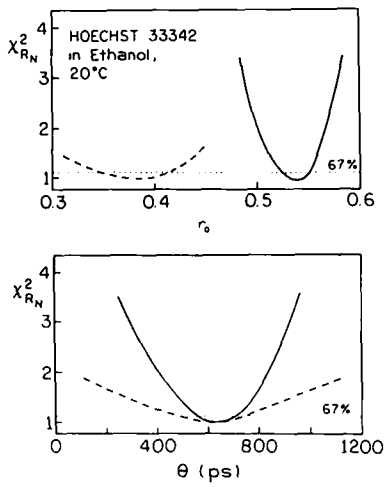

Fig. 5. χ^2_R surfaces of correlation times and limiting anisotropies for one-photon (---) and two-photon (——) excitation.

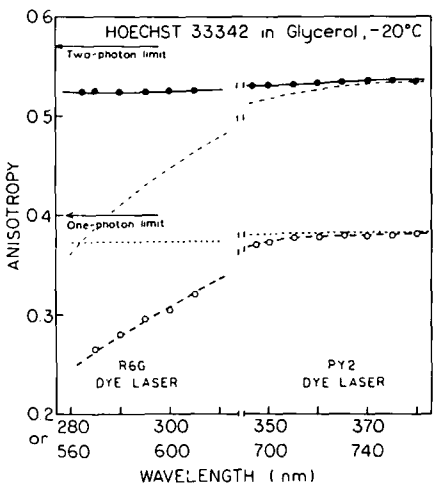

Fig. 6. Excitation anisotropy spectra of Hoechst 33342 in glycerol, −20°C. The upper dashed line shows the anisotropy values expected for an increased TPE photoselection factor of 10/7.

−20°C (Fig. 6). For excitation with the lowest singlet state (OPE, 345–380 nm; TPE, 690–760 nm), the anisotropy values are almost exactly related by the factor 10/7. In the shorter wavelength range (OPE, 285–310 nm; TPE, 560–620 nm), where some excitation to the S_2 state probably occurs, the OPE anisotropy values decrease with wavelength (Fig. 6; ooo), whereas the TPE values remain high and constant (●●●). This result suggests that OPE results in some excitation to a different (higher) electronic state, where the absorption and emission oscillators are less colinear. For TPE, these oscillators remains colinear, which suggests that the S_0–S_2 transition has a lower two-photon cross section.

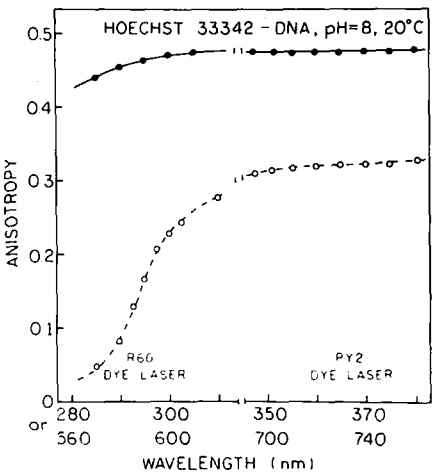

Fig. 7. Excitation anisotropy spectra of the Hoechst 33342–DNA complex.

Anisotropy Excitation Spectra of the Hoechst 33342–DNA Complex

We also examined the anisotropy spectra of HOE when bound to DNA (Fig. 7). In this case, the steady-state anisotropy values decreased rapidly for OPE below 300 nm. This wavelength coincides with the onset of the DNA absorption, so it seems likely that the decrease in anisotropy is due to energy transfer from the DNA bases to HOE. Surprisingly, the TPE anisotropy values do not decrease in this range of wavelength, which suggests that the relative cross section for two-photon absorption of DNA is smaller for TPE than for OPE.

CONCLUSIONS

Hoechst 33342 displays a high cross section for two-photon absorption in the wavelength range from 560 to 760 nm (~10^{-48} cm^4 s/photon molecule). The anisotropy remains high over this wavelength range, suggesting that there is a dominant two-photon cross transition with colinear absorption and emission oscillators. Hoechst 33342 displays essentially the same lifetimes and correlation times for OPE and TPE, which will allow direct comparison of the one-photon and two-photon experimentation data. And finally, the TPE of Hoechst 33342 appears to be possible without two-photon absorption of DNA.

These results suggest that Hoechst 33342 is a useful probe for two-photon spectroscopy and microscopy and that one can directly compare the one- and two-photon experiments.

ACKNOWLEDGMENTS

This work was supported by grants from the National Science Foundation (MCB-8804931 and DIR-8710401) and the National Institutes of Health (GM 39617 and RR-08119).

REFERENCES

1. S. A. Latt and G. Stetten (1976) *J. Histochem. Cytochem.* **24**, 24–30.
2. I. W. Taylor (1980) *J. Histochem. Cytochem.* **28**, 1021–1027.
3. J. Kapuscinski (1990) *J. Histochem. Cytochem.* **38**, 1323–1329.
4. D. J. Arndt-Jovin and T. M. Jovin (1977) *J. Histochem. Cytochem.* **25**, 585–590.
5. E. S. Critser and N. L. First (1986) *Stain Technol.* **61**, 1–9.
6. H. M. Shapiro (1981) *Cytometry* **2**, 143–151.
7. M. Poot, T. J. Kavanagh, H. C. Kang, R. P. Haugland, and P. S. Rabinovitch (1991) *Cytometry* **12**, 184–192.
8. F. Otto and K. C. Tsou (1985) *Stain Technol.* **60**, 7–16.
9. A. Bernheim and R. Miglierina (1989) *Hum. Genet.* **83**, 189–196.
10. D. J. Arndt-Jovin and T. M. Jovin (1990) *Cytometry* **11**, 80–88.
11. J. R. Quintana, A. A. Lipanov, and R. E. Dickerson (1991) *Biochemistry* **30**(42), 10294–10306.
12. C. H. Chen, A. Mazumder, J. F. Constant, and D. S. Sigman (1993) *Bioconjugate Chem.* **4**(1), 69–77.
13. S. Kumar, T. Joseph, M. P. Singh, Y. Bathini, and J. W. Lown (1992) *J. Biomol. Struct. Dynam.* **9**(5), 853–880.
14. A. Fede, A. Labhardt, W. Bannwarth, and W. Leupin (1991) *Biochemistry* **30**(48), 11377–11388.
15. J. R. Lakowicz, I. Gryczynski, E. Danielsen, and J. K. Frisoli (1992) *Chem. Phys. Lett.* **194**, 282–287.
16. J. R. Lakowicz and I. Gryczynski (1993) *Biophys. Chem.* **45**, 1–6.
17. J. R. Lakowicz, I. Gryczynski, J. Kusba, and E. Danielson (1992) *J. Fluoresc.* **2**, 247–258.
18. J. R. Lakowicz and I. Gryczynski (1992) *J. Fluoresc.* **2**, 117–121.
19. M. J. Sepaniak and E. S. Yeung (1977) *Anal. Chem.* **49**, 1554–1556.
20. M. J. Wirth and F. E. Lytle (1977) *Anal. Chem.* **49**, 2954–3057.
21. R. R. Birge (1986) *Acc. Chem. Res.* **19**, 138–146.
22. S. P. Jiang (1989) *Prog. React. Kinet.* **15**, 77–92.
23. A. A. Rehms and P. R. Callis (1987) *Chem. Phys. Lett.* **1490**, 83–89.
24. W. Denk, J. H. Strickler, and W. W. Webb (1990) *Science* **248**, 73–76.
25. D. W. Piston, D. R. Sandison, and W. W. Webb (1992) *Proc. SPIE* **1640**, 379–389.
26. S. M. Kennedy and F. E. Lytle (1986) *Anal. Chem.* **58**, 2643–2647.
27. J. R. Lakowicz, H. Szmacinski, K. Nowaczyk, K. Berndt, and M. L. Johnson (1992) *Anal. Biochem.* **202**, 316–330.
28. J. R. Lakowicz, H. Szmacinski, K. Nowaczyk, and M. L. Johnson (1992) *Cell Calcium* **13**, 131–147.
29. Molecular Probes Catalogue, Molecular Probes, Eugene, OR.
30. J. R. Lakowicz, G. Laczko, and I. Gryczynski (1986) *Rev. Sci. Instrum.* **57**, 2499–2506.
31. G. Laczko, I. Gryczynski, Z. Gryczynski, W. Wiczk, H. Malak, and J. R. Lakowicz (1990) *Rev. Sci. Instrum.* **61**, 2331–2337.
32. J. R. Lakowicz, I. Gryczynski, Z. Gryczynski, E. Danielsen, and M. J. Wirth (1992) *J. Phys. Chem.* **96**, 3000–3006.